ORGANISATION EUROPEENNE POUR LA RECHERCHE NUCLEAIRE
EUROPEAN ORGANIZATION FOR NUCLEAR RESEARCH

Laboratoire Européen pour la Physique des Particules
European Laboratory for Particle Physics

17 November 2006

Design, Construction and Metrology of the Overlap Detectors for the ALFA system

A. Braem[a], C. David[a], A. Folley[a], C. Joram[a], L. Kottelat[a], A. Mapelli[a,b,*], M. van Stenis[a], H. Stenzel[c], M. Szauter[c]

[a] *CERN, PH Department, CH-1211 Geneva, Switzerland*

[b] *EPFL, LMIS4, CH-1015, Lausanne, Switzerland*

[c] *II. Physikalisches Institut, Justus-Liebig-Universität, Giessen, Germany*

ATL-LUM-PUB-2007-004
11 June 2007

Abstract

We present the design and construction of a prototype overlap detector for the alignment of the ALFA scintillating fibre tracker. The full system has been developed and built for beam tests at the CERN SPS H8 in autumn 2006.

1. Introduction: The ALFA 2006 prototype overlap detectors

The ALFA detector [1] is a scintillating fibre tracking detector proposed for the absolute determination of the LHC luminosity at the ATLAS interaction point (IP1). This detector will track protons elastically scattered under μrad angles at IP1. It will be placed at 240m on each side of the main ATLAS detector at CERN. The position of the LHC beam spot at these locations is a priori unknown and can vary from fill to fill up to a couple of mm. It is therefore necessary to position the upper and lower ALFA detectors symmetric to the beam spot before a meaningful measurement can start. Simulations [2] have shown that the vertical distance between the two ALFA half detectors must be known with a precision of about 10 μm. The approach chosen to determine this distance is the so-called overlap detectors. The overlap detectors (ODs) are particle detectors that need to measure only the vertical coordinate. Two ODs are mounted below and above the actual detector planes.

The distance of the detector halves can be calculated from the measurement of particles which traverse both ODs:

$$d = \sum_{i=1,N} \left(y_i^1 - y_i^2 \right) \tag{1}$$

where N is the total number of particles that have hit both detectors, y_i^1 and y_i^2 are the y-coordinate of the hit for one of the ODs and for the other. The required measurement precision is obtained by recording a sufficiently large number of tracks and calculating their average in the two ODs. The achievable precision depends on three factors: the intrinsic spatial resolution of the OD, the statistics of particles detected with the OD and the alignment uncertainty between the ODs and the detector halves.

* Corresponding author: Alessandro.Mapelli@cern.ch

Ideally the overlap measurements are made with 7 TeV protons which are transported parallel to the primary beam. Therefore, as shown in the drawing of Figure 1, the overlap detectors should be included inside the aperture of the beam tube with a diameter of 50 mm, moreover it should be within the aperture of the beam screen which at this position has a horizontal diameter of 44 mm. Outside this limit the composition of the beam halo may be dominated by shower particles originating from hadronic interactions of the beam with collimators and structural components.

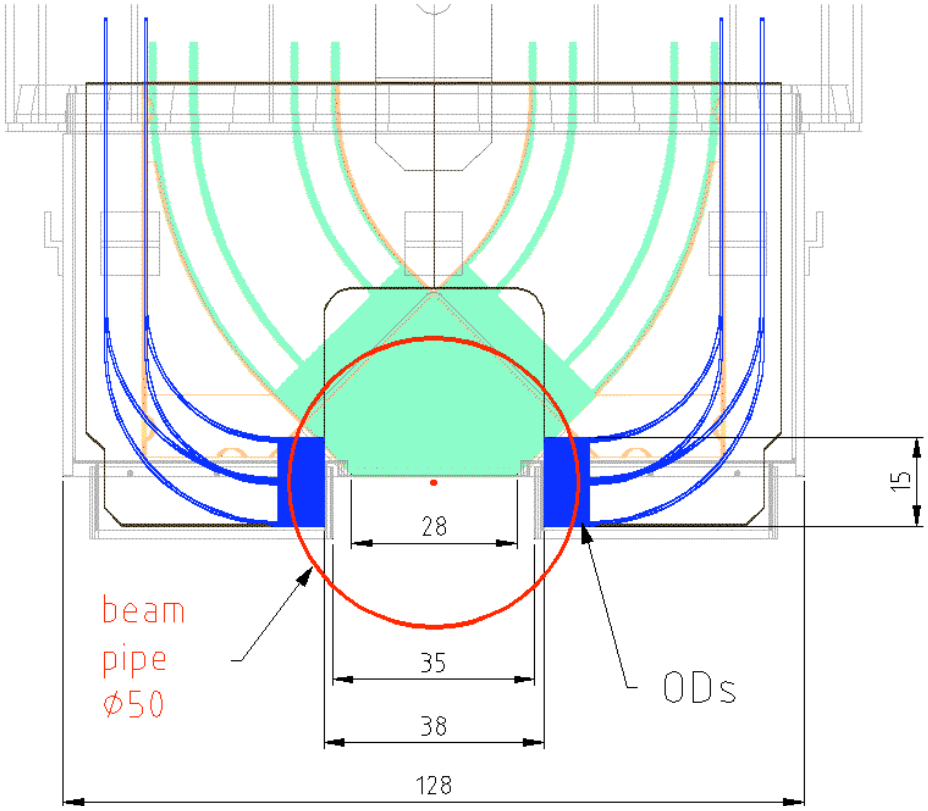

Figure 1: Front view of the full detector assembly with the overlap detectors. The spot and the circle in the centre represent the beam axis and the beam tube. Not shown are the beam screens which have at this position a horizontal diameter of 44mm.

The overlap detectors consist of horizontally mounted scintillating fibres[1] of the same type and size as the main detector. They cover an active area of 6×15 mm^2. An OD comprises 3 planes of 30 fibres. A complete description of the overlap detector can be found in reference [2]. To verify the concept and to demonstrate the achievable resolution a prototype detector was designed and tested in a high-energy beam[2] at SPS-H8 CERN. The number of available MAPMT channels (320) in the test beam did not allow to test a configuration with an effective pitch of 166 µm as this would have required 3 planes per OD and a total number of 360 fibres. Two identical sets of two planes each were built. The two planes were vertically staggered by 250 µm (half the size of the fibre). Thus the effective pitch of the detector was 250 µm. The horizontal fibres were bent by 90° and routed upwards to the MAPMTs. In order to maximize the bending radii of the fibres, the 30 fibres were split into two layers of 15 fibres mounted on the front and on the back side of a ceramic support plate.

The two prototype ODs were mounted on the same support arm at a distance of 50 mm from each other. The upstream detector (OD2) was mounted on a micrometric translation table whereas the downstream detector (OD1) was mounted statically on the support arm. With this simple set-up OD2 could be displaced vertically relative to OD1.

[1] Single cladded 0.5 mm square fibre SCSF-78, S-type, from Kuraray, Japan

[2] π, p up to 230 GeV/c

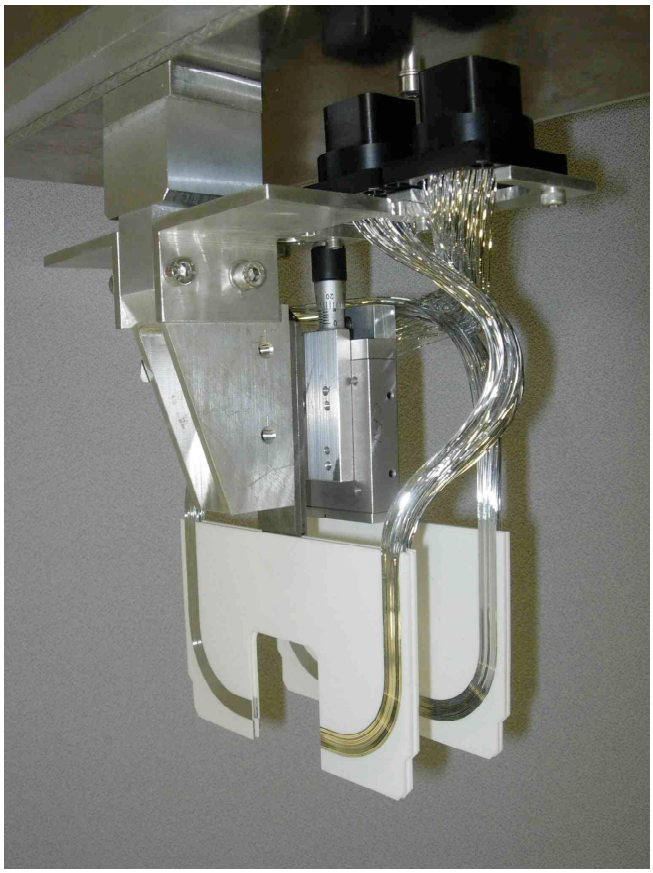

Figure 2: Picture of the prototype overlap detectors for beam tests. Back side of the plates are shown.

The ODs provided the coordinate information in discrete steps of 500 µm / 2 = 250 µm. The difference of the hits in the two detectors could also be measured only in discrete steps of 250 µm. Differences smaller than 250 µm were derived by averaging the measured discrete differences over a sample of events with sufficiently large statistics (see Equation 1).

2. Bending the scintillating fibres

The overlap detectors have an active area of 6×15 mm^2 on each side (left and right) of the ALFA detector; they have been designed to keep the first 8mm of the fibres straight and horizontal. Great effort was put during all the steps of the production to keep this segment straight and unaltered especially during the bending process. The fibres had to be bent to radii going from 22.5 mm for the most inner fibre to 30 mm for the most outer. However previous tests [3] showed that bending scintillating fibres at room temperature at radii of 15-30mm lead to significant degradation of their light transport performance due to the formation of cracks. Light transmission along a cracked fibre is dramatically reduced because light escapes from the cracks or is reflected and propagates on the opposite direction. The picture of Figure 3 shows a cracked scintillating fibre excited with blue light. The spot in the middle of the fibre is light escaping from a crack. The plot in Figure 4 shows how light transmission in a cracked fibre degrades. In order to bend the fibres to smaller curvature radii than specified by the manufacturer, a temperature cycle was defined.

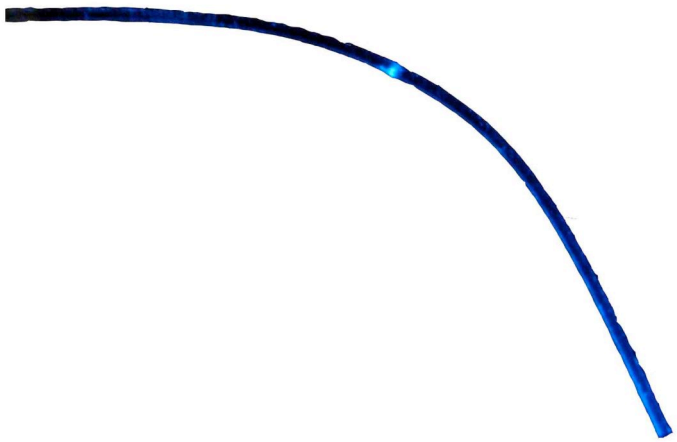

Figure 3: Fibre bent at room temperature. The clear spot is a crack from where light escapes.

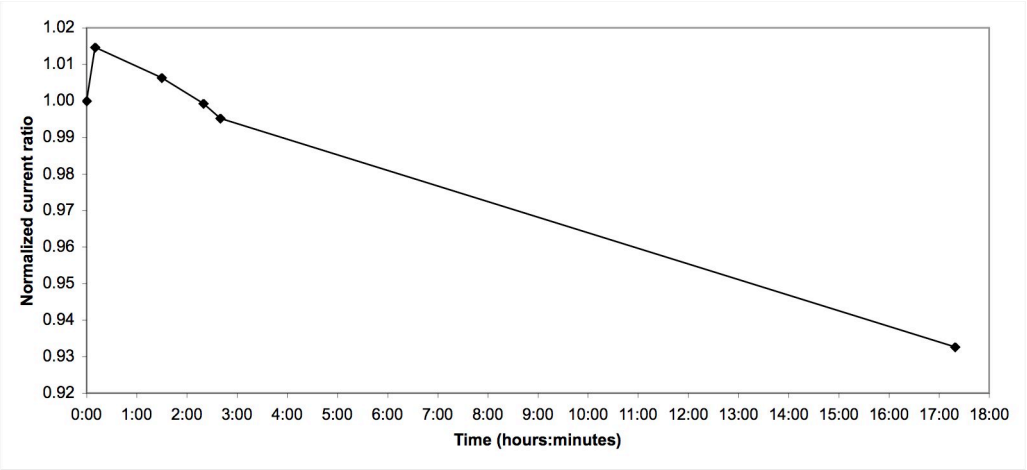

Figure 4: Photocurrent ratio for a fibre bent at room temperature normalized to 1. After a small increase, the ratio decreases with time due to cracks forming in the bent part of the fibre.

The setup shown in Figure 5 was used to test the influence of temperature on fibres while bending them. It allowed to blow air at different temperatures on a single fibre while bending it at a radius of 15mm at different temperatures. A Pt-100 sensor measured the temperature of the air blown on the fibre.

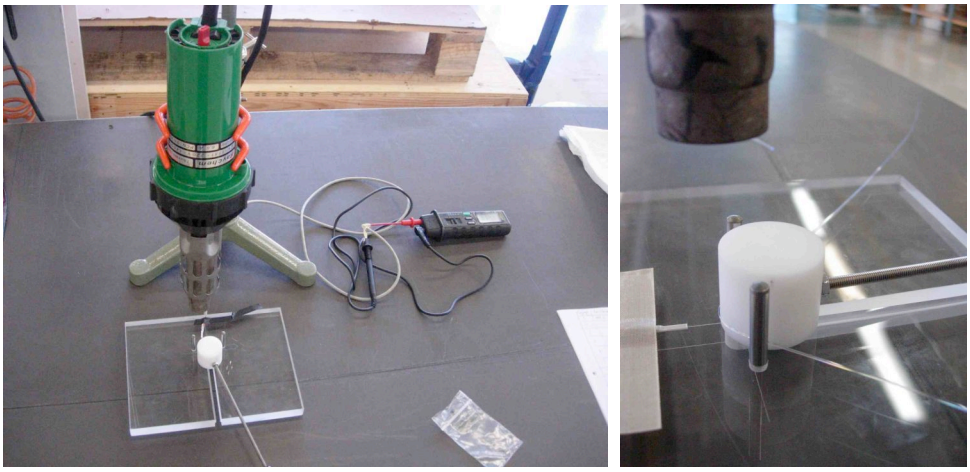

Figure 5: Setup used to bend single fibres at different temperatures.

Every bent fibre was visually inspected and light transmission tests were performed. To determine the degradation induced by the bending of the fibre, the light transmission of the same fibre was compared before and after bending it. The tests were carried out on 30 cm long fibres. Their ends were cut with a pliers and polished. Each measurement was performed twice, measuring the light with a silicon photodiode[3] from one side of the fibre and then the other to minimize the effect of possible superficial inhomogeneities. The result was obtained by averaging the two measurements. The light was injected in the fibre by the side at two different points (see Figure 6) and the ratio of the resulting photocurrents was compared for the same fibre before and after bending. A blue LED[4] was used to excite the wavelength shifter in the core of the fibre. A small opening of 0.5×0.5 mm^2 on a black Plexiglas block confined light and the fibre was inserted in the block through a channel. This way all the measurements were done with the same excitation light intensity. When bending the fibres at temperatures comprised between 80°C and 100°C the light transmission did not drop off and sometimes even increased. In this range of temperature the bending angle was approximately 90° (see Figure 7).

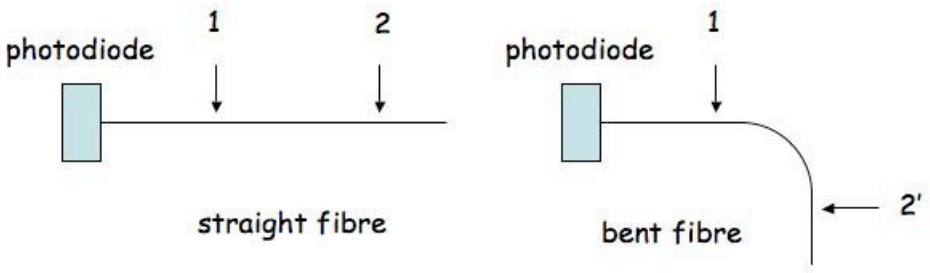

(a) (b)

Figure 6: Schematic drawing of the light transmission tests performed (a) before and (b) after bending the fibre. Fibres were excited at the same two points before and after bending.

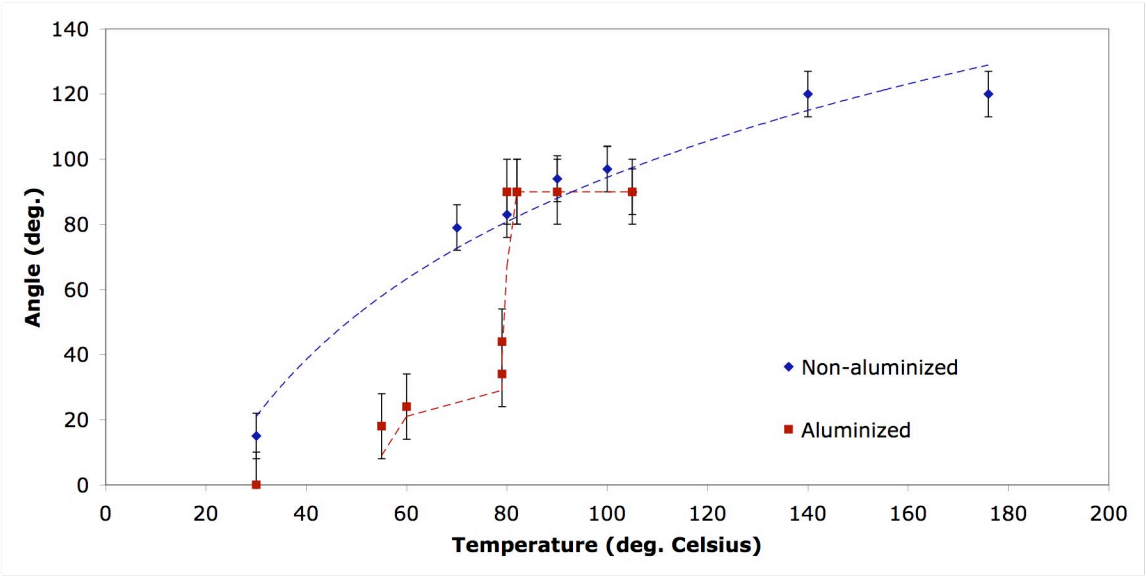

Figure 7: Angle of the fibre as a function of the bending temperature.

The optical transmission of the fibres bent between 80°C and 100°C was slightly improved as seen on the plot of Figure 8. In this temperature range the normalized ratio of the photocurrents of the same fibre is bigger than one. This increase could indicate the presence of minor changes in the superficial reflectivity due to heating. The interface between the core of the fibre and its cladding or the structure of the materials

[3] Newport 818-UV
[4] Bivar, LED5-UV-400-30 Series

itself might have been altered by the temperature treatment. Over 100°C, these alterations became such that the transmission was deteriorated. The fibres bent at room temperature did not deteriorate at first (just a few %) but after twenty days they had lost most of their optical transmission. This can be explained by the fact that cracks appeared immediately as the fibre was bent, inducing a small decrease in the transmission. Once removed from the tool and even though they got back to an almost straight position, cracks in the fibres propagated degrading their optical properties. Above 100°C the fibre is deformed in all directions; it does not stand such a high temperature.

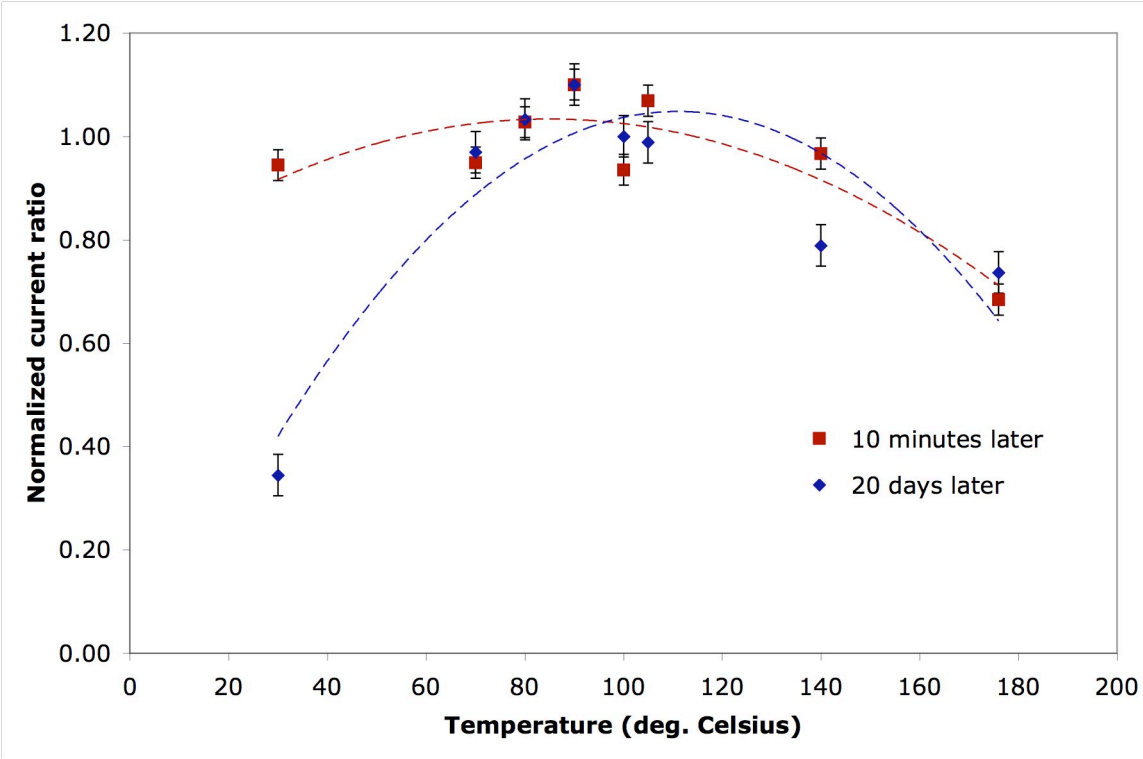

Figure 8: Ratio of the photocurrents before and after bending of the fibres. The photocurrents were measured on straight fibres and on bent fibres 10 minutes after they had been bent and 20 days later. The photocurrents decreased for the fibres bent at temperatures lower than 80°C and higher than 100°C.

Complementary tests were performed with improved tooling and the 240 fibres for the prototype ODs were bent in a Teflon tool by batches of 30 as shown in the pictures of Figure 9.

The fibres were held in the tool by lightly compressing them on two points by a Viton joint. A thin film of Tedlar prevented the joint from damaging the Al-coating. Both the Viton joint and the Tedlar film are produced by Dupont[5]. Three batches of ten fibres were arranged in three channels 0.5mm deep and 5mm wide machined in a slab of Teflon. One end of the tool was machined at a radius of 22.5 mm. The 35 mm to be bent were left hanging and the last 8mm were placed in a channel and covered with a block of Teflon to keep them straight while heating the rest of the fibre. The temperature was ramped up from room temperature to 85°C in twenty minutes to reach the temperature of plastic deformation of the fibres and avoid stressing them by bending them abruptly. The fibres were then gently bent around the tool and gently held with a Teflon cap screwed on the tool. The bent part of the fibre was covered and kept at 85°C for twenty minutes, after which the cap was removed and the fibres were still left at 85°C for fifteen minutes. The temperature was then ramped down to room temperature and the fibres were removed from the tool.

With this procedure the fibres for the prototype overlap detector have been bent to an angle of 90°. Different angles could be obtained according to the time during which the fibres were left at 85°C.

[5] du Pont de Nemours and Company

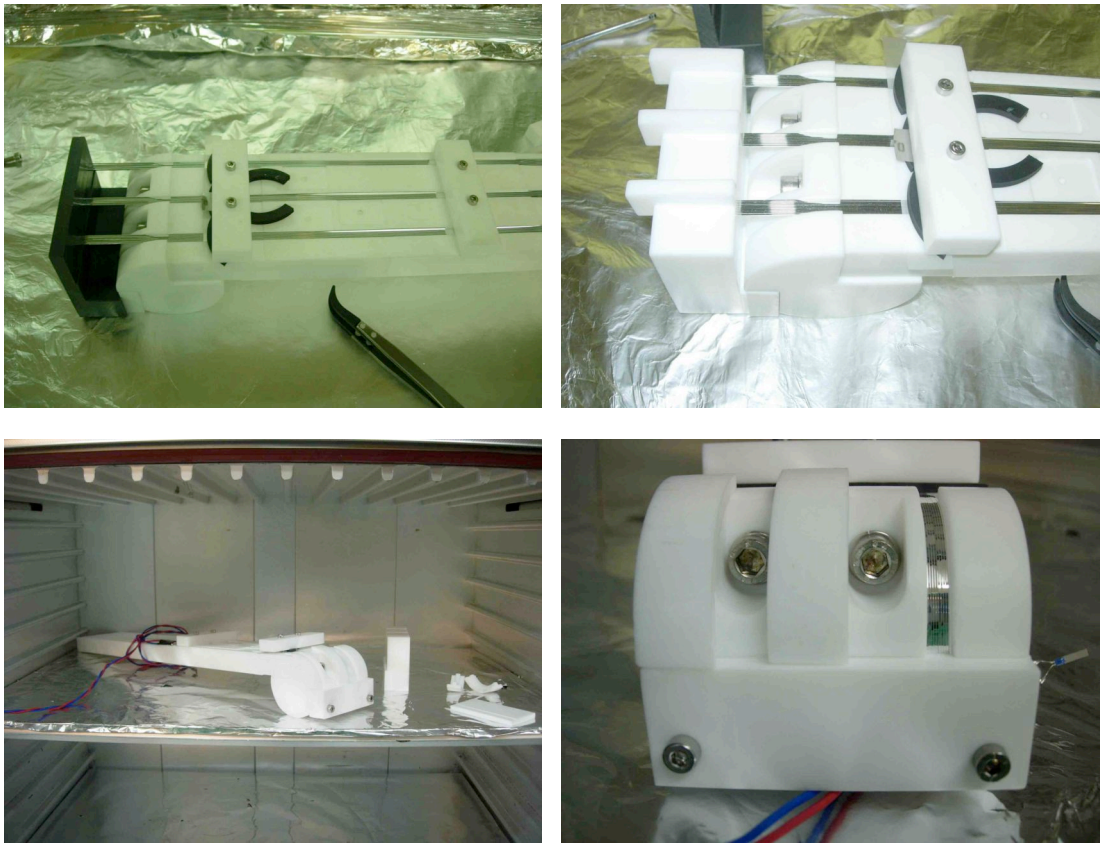

Figure 9: Setup used to bend the overlap detectors fibres in an oven. 3×10 straight fibres are placed in the tool and held by Teflon blocks. Once they have reached 85°C they are bent and kept in position for twenty minutes. When the tool has reached room temperature fibres are removed from it.

3. Fibres glueing on the ceramic substrates

Different steps of the glueing of the bent fibres are shown in the pictures of Figure 10, the ceramics plates were held on a metallic support by two Teflon blocks and one lever. Another block was pushed against the inner side of the opening in the ceramic plates to align the fibre ends.

A thin layer of glue[6] was spread along the ceramics inner plate's edge and on the main substrate over a width of 2.5 mm to position the horizontal section of the five upper fibres. This step was repeated two more times until the fifteen fibres were in place. Two arms were then set on top of the fibres to keep them from overlaying one another. The first fibre (the most upper one) was gently pushed against the vertical edge of the inner ceramic plate. Then the second one was positioned against the first and so on until the fifteen fibres were tightly glued to each other. A small ceramic piece was glued on the main ceramic substrate in order to constrain the fibres against the edge of the central ceramic plate. This small ceramic piece was pushed against the fibres by four Teflon blocks. The excess glue was gently swept away from the fibres with a tissue of class 100 and methanol. On top of the fibres were placed two Teflon blocks with an extra load to push the fibres against the ceramic plate while the glue polymerized. The fibres were left like this until complete polymerization of the glue and then the holding blocks were removed. This was repeated for the 60 fibres of every plate.

[6] Bicron BC-600 optical cement

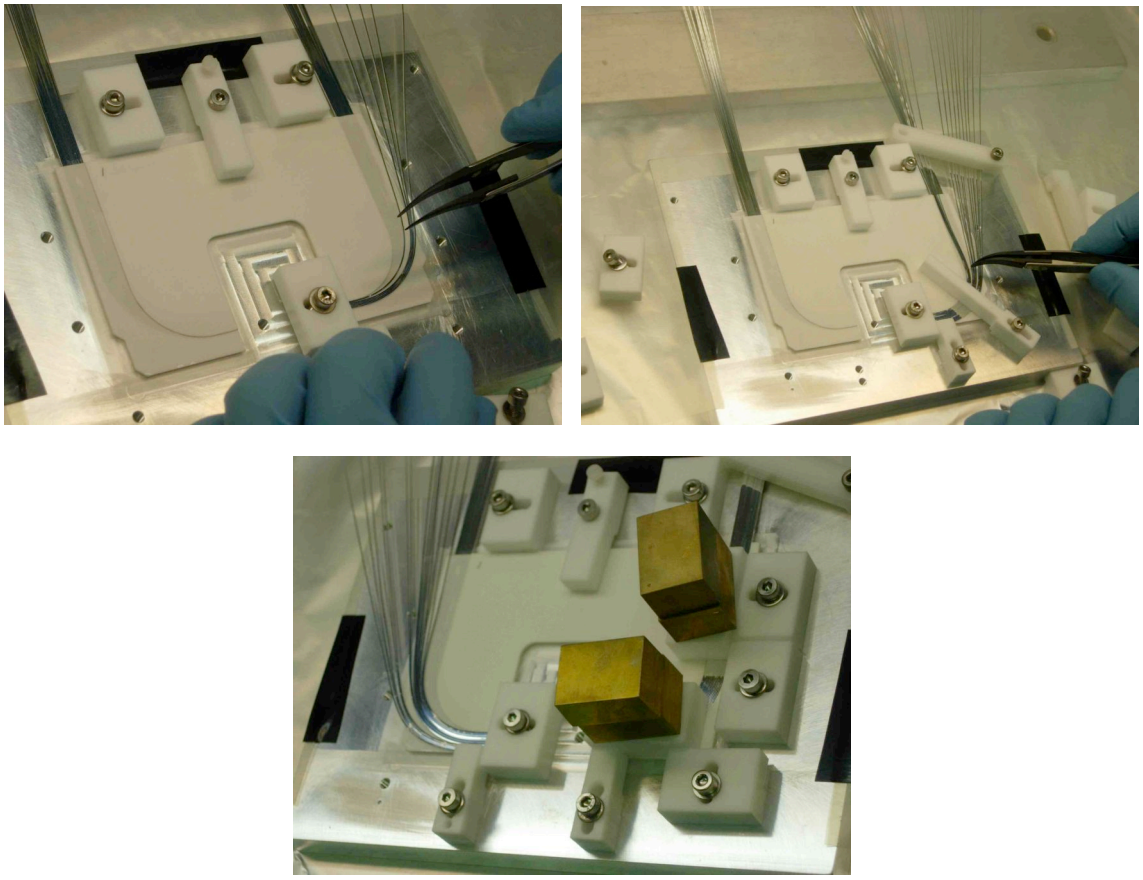

Figure 10: Pictures of the glueing of the fibres on the ceramic substrates. The ceramic substrate is held in the tool and glue is spread over it. The fibres are then precisely positionned one by one. Some loads are put on top of the fibres to hold them in place while the glue polymerises.

4. Construction

The sequence of steps for the construction of the overlap detectors was the following:

1. LASER cutting in industry of the central and stiffener plates from Al_2O_3 ceramic sheets at a precision of about ±30 µm.
2. Glueing of the ceramic plates.
3. Machining and Al-coating of the fibre ends (details about steps 3 and 4 can be found in reference [4]).
4. Al-coating of the fibre sides.
5. Bending of the Al-coated fibres following a temperature cycle. The fibres were pre-heated to their temperature of plastic deformation to release inner constraints; they were subsequently bent and left in the tool at constant temperature. 30 fibres were bent at a time.
6. Positioning and glueing of the fibres. The fibre ends are aligned and the outer stiffener plate gently compresses the fibres.
7. Survey for control of the fibre position, pitch and angle.
8. Glueing of the support blade made of hardened steel. The position of the blade was chosen to produce the desired staggering. This step was done by means of an alignment plate that provided a specific position for each displacement and allowed also to (partly) correct for small geometrical errors accumulated in the sequence up to this step.
9. Survey of fibres positions and angles relative to the precision holes of the steel blade.
10. Assembly of the two planes of OD1 on a support arm through two precision pins.
11. Assembly of the two planes of OD2 on a translation table fixed on the support arm holding OD1.

12. Threading of the fibres into the connector and subsequent glueing. A system has been adopted which avoids that adjacent fibres on the detector are not connected to adjacent channels on the MAPMT[7].
13. Machining with a diamond tool of the protruding fibre ends of the connectors.

Optical cement Bicron BC-600[8] was used to glue both fibres and ceramic components.

The prototype overlap detectors were tested in a lab set-up where the fibres were exposed to an Sr-90 source and read out by an MAPMT. These tests are presented at the end of this document. They showed that the light of the heated and bent Al-coated fibres of the overlap detectors gave the same light yield as the straight Al-coated fibres glued on the other ALFA detectors.

5. Metrology

During its construction the overlap detector prototype was measured three times with an optical coordinate measurement machine[9] (CMM). Details about the machine can be found in reference [5]. The first survey asserted the fibre position on the ceramic plates. The second survey was required to precisely position the metallic blade w.r.t. the ceramic plates. To do so, the blade was positioned on a tool with two precision pins and the centre of the upper pin was defined as the origin of the two axis used to re-measure the fibre positions as shown in Figure 11. The centre of the oblong hole of the blade was chosen as a second point to define the *y-axis*. The ceramic plate was then positioned against three precision pins C1, C2, C3.

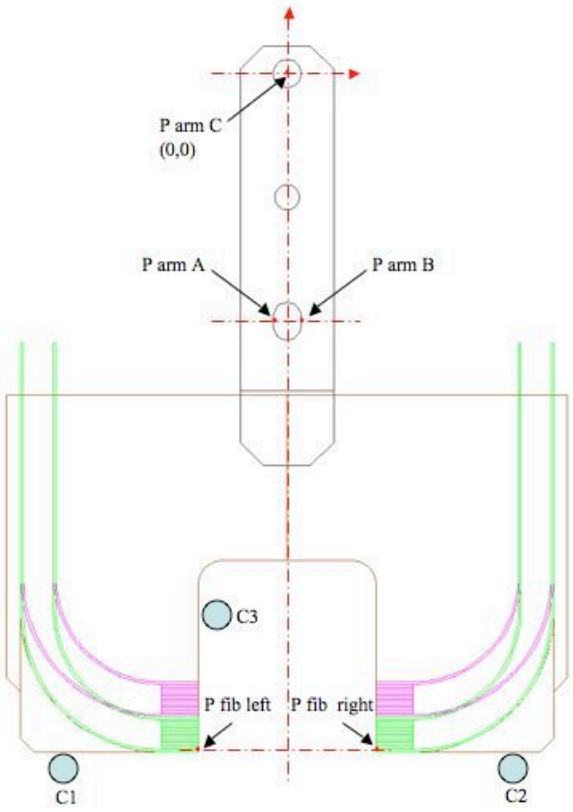

Figure 11: Design of one plate of the ODs under measurement for the glueing of the blade on the ceramic plate.

The end points of the lower two fibres were measured on each side of the plate. These two points defined a straight line and a spacer was inserted between the plate and pin C3 to move the plate such that the centre of this line would stand at *x=0*. The plate was then rotated in order for the fibres to be

[7] Model R7600 from Hamamatsu Photonics, Japan
[8] Saint-Gobain Ceramics & Plastics, Inc.,
[9] SmartScope CNC 250, OGP Inc.

perpendicular to the blade's vertical axis (the *y-axis*). This rotation was achieved by placing a spacer between the plate and either pin C1 or C2 according to the angle to be corrected. Finally, identical spacers were inserted between the plate and spacers C1 and C2 to place the fibres at the required height. The position of each blade relative to the plates was chosen to produce the desired vertical staggering.

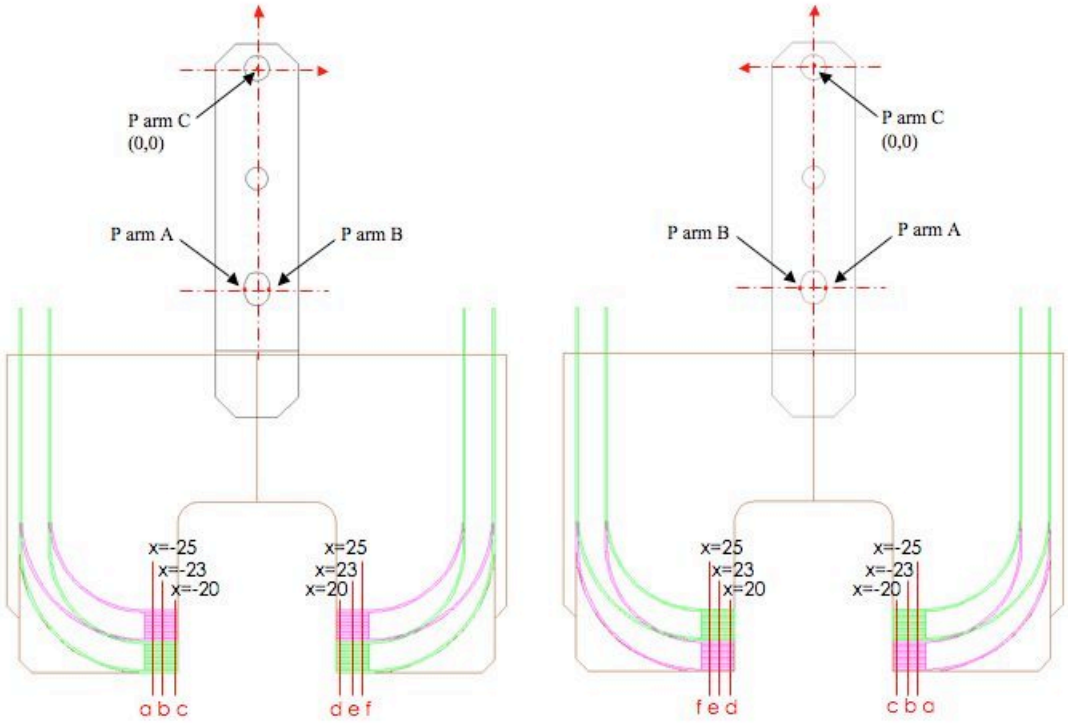

Figure 12: Metrology procedure for the final survey of the four overlap detector plates to determine the fibres position.

To determine the exact position of the fibres, the y-coordinate of the gap between the fibres was measured at three different x positions (20, 23 and 25 mm from the centre of the system) as drawn in Figure 12. The pitch and the centre of the fibres were determined and the slopes calculated (Figure 13 and Figure 14). Within a layer the slopes of all the fibres have a small variation but from one layer to the other there can be large variations. Moreover from the plot of Figure 14 it is clear that the pitch of all the fibres is very close to the expected 500 µm except for fibre 16 of every layer. These two geometrical effects come from the imprecise alignment of the upper fibre on the front side of the substrate and the lower fibre on the back side. The positioning of the fibres on each side of the detector is done relative to the inner ceramic plate's lower edge, thus within the layer the pitch is well controlled but not from one side to the other. This imperfection has to be corrected in the next prototype. The staggering between the fibres of OD2 and OD1 is plotted in Figure 15. Its mean value is less than 10 µm away from the expected value of 250 µm (fibre size divided by the number of plates per OD, namely two) but it goes as far as 350 µm. The variation in the staggering comes from the accumulation of the small displacement of every fibre during the glueing. Good care must be taken during this step of the construction sequence.

This geometrical data was recovered in a geometry file that was used to simulate the detector in a beam and to reconstruct real events from the test beam that took place in October 2006 at CERN.

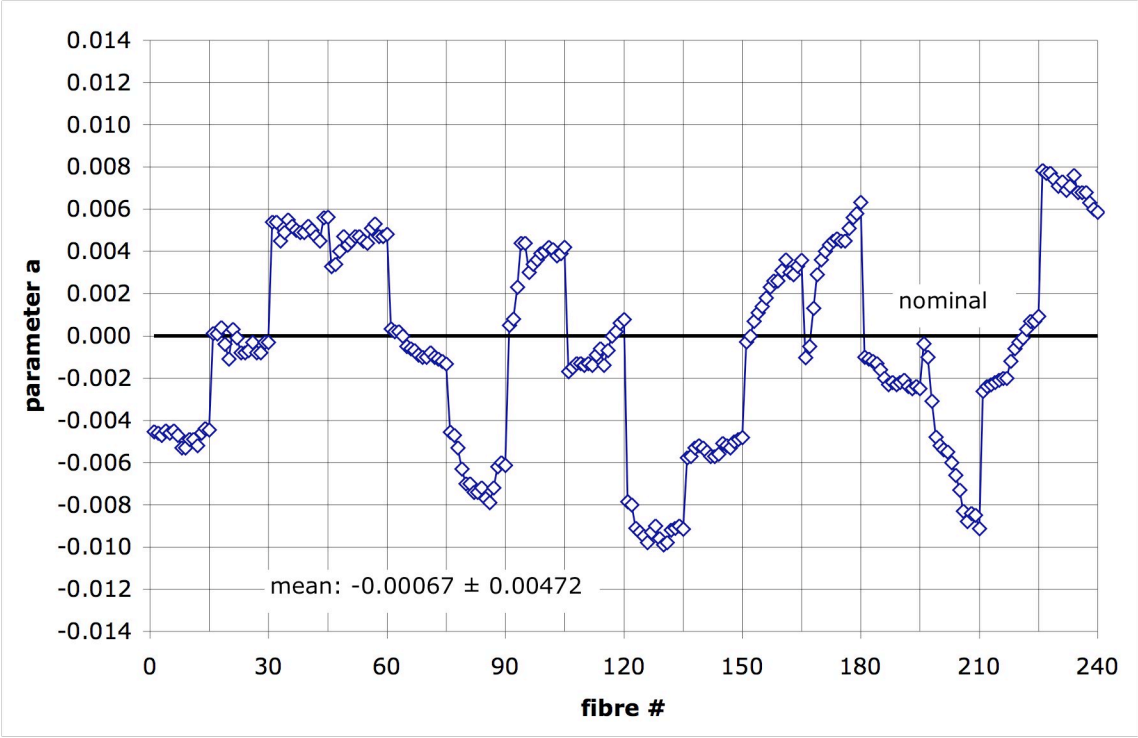

Figure 13: Parameter *a* (fibre slope) for all fibre of the overlap detector.

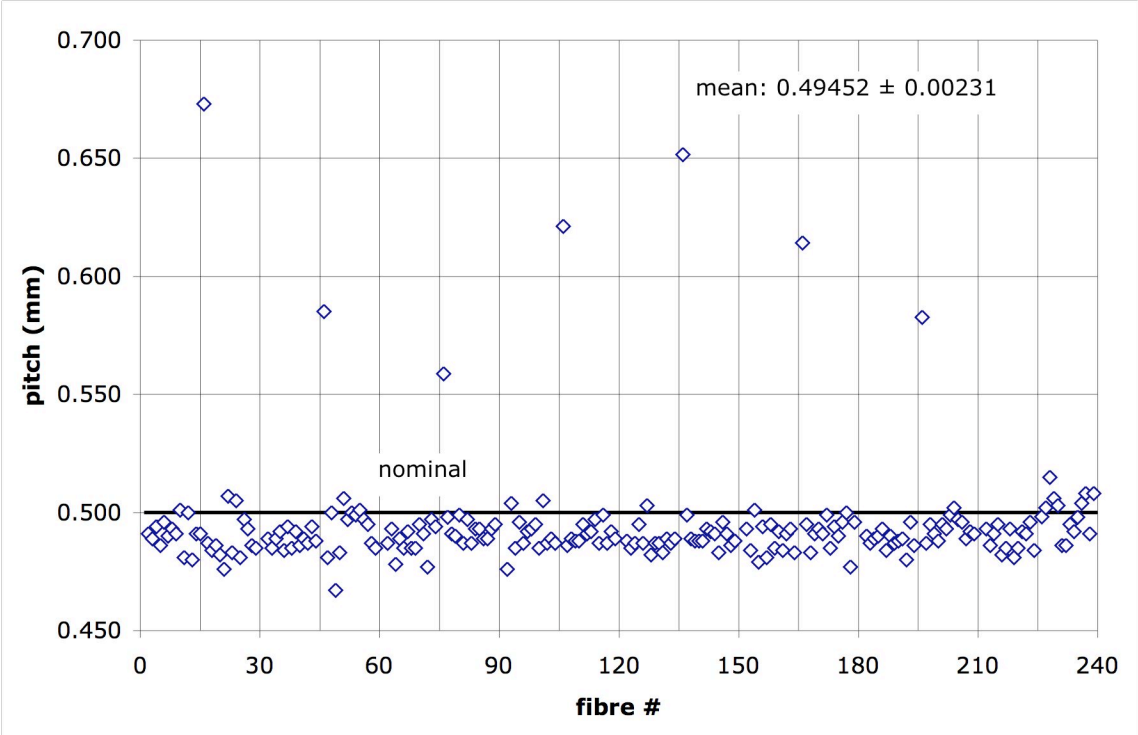

Figure 14: Fibre pitch for the overlap detector.

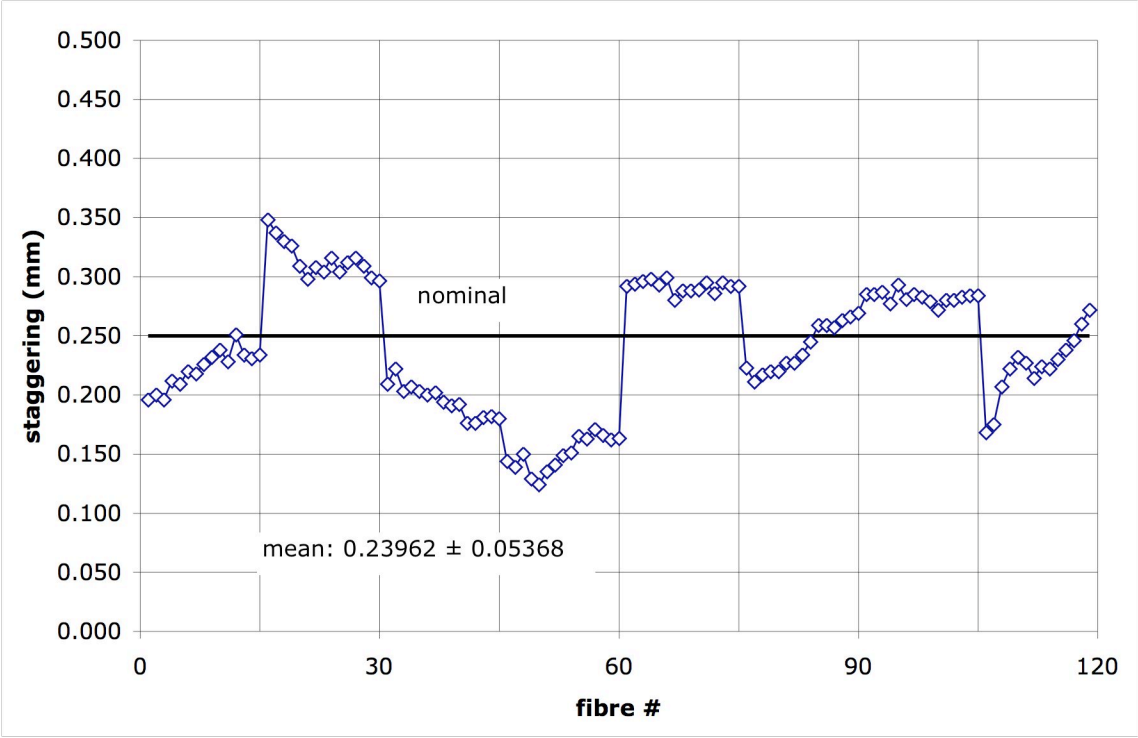

Figure 15: Staggering between fibres of the two plates of OD2 and OD1.

6. Simulation studies

To estimate the achievable vertical resolution σ_y, particle tracks were generated with a simple geometrical Monte-Carlo code and the hits with the detector were reconstructed taking into account the measured fibres geometry. The code uses the average algorithm to reconstruct the y-coordinate of the particle. The reconstruction algorithm was derived from equation 1:

$$y_{rec} = \frac{1}{2}\left(y_{OD1,L1} + y_{OD1,L2}\right) - \frac{1}{2}\left(y_{OD2,L1} + y_{OD2,L2}\right) \tag{2}$$

where $y_{ODi,Lj}$ is the coordinate of the fibre hit in the jth layer of the the ith overlap detector. The plots of Figure 16 show the residual reconstructed coordinate relative to the hit coordinate. The standard deviation of these box plots gives us the resolution we can expect from each overlap detector with their measured geometry. The theoretical resolution of the ODs, taking into account the inactive cladding of the fibres, is 240 µm / √12 = 69 µm. Simulating the ODs with a detection efficiency of 95% resulted in a resolution of 69 µm for OD1 and 73 µm for OD2. Effects such as cross-talk or multiple scattering were not simulated; the divergence between the theoretical and simulated resolution of OD2 is attributed to geometrical imperfections.

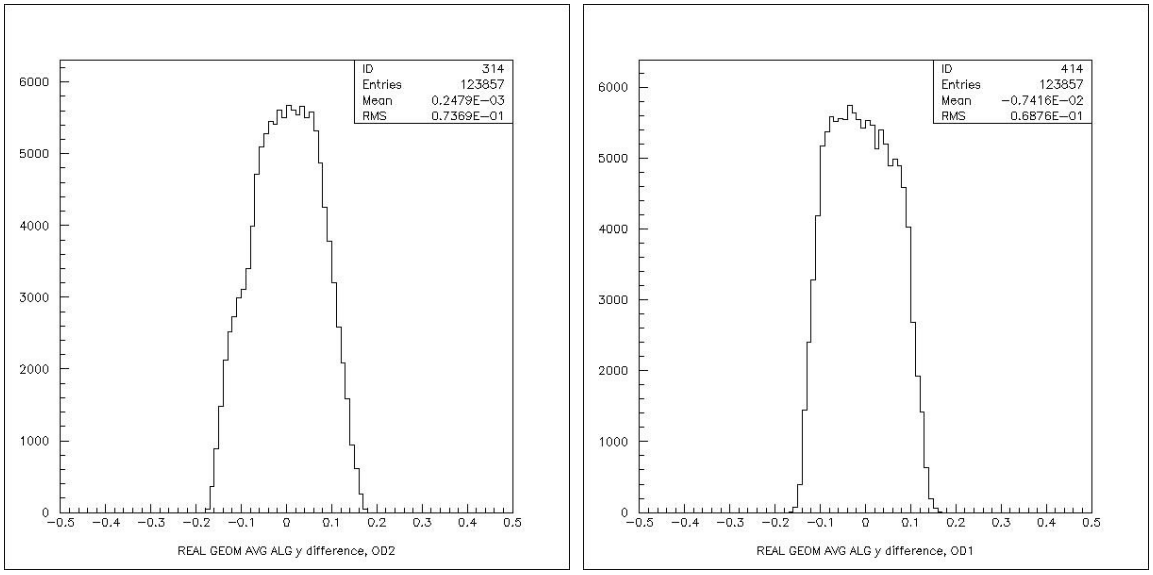

(a) (b)

Figure 16: Result of a Monte-Carlo study using the 'as measured geometry' for (a) OD2 and (b) OD1 (b).

7. Tests of the prototype detector

Tests were performed on the fibres to determine their light yield after different steps of the construction sequence. The light yield of processed fibres was compared to the yield of non-aluminized straight fibres and the average light yield of the mounted ODs' fibres was compared with the average light yield of the fibres from other ALFA detectors.

The following fibres were tested; non-aluminized straight fibres, non-aluminized bent fibres, Al-coated straight fibres, Al-coated bent fibres. The fibres end was in contact with the window of a PMT[10] and an Sr-90 source was placed over one side of the fibres close to the other end. The measurements were done at U_{PMT} = 1200V; triggering was done on the fibre signal itself. The light yield was calculated for 15000 events:

$$N_{pe} = ENF\frac{Q^2}{\sigma_Q^2} \tag{3}$$

where:

ENF is the excess noise factor of the PMT and is assumed to be 1.4,

Q is the output charge,

σ_Q is the standard deviation of the response pulse.

The different fibres gave a light yield of approximately 2.8 photoelectrons as shown in the screen capture of Figure 17. The absolute number of photoelectrons may be not very precise with this method. However the comparison of the four sets of fibres validates the process.

[10] EMI 9826A

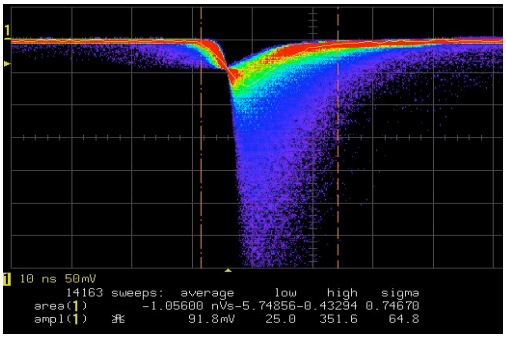

Figure 17: Output pulse of the PMT connected to a single fibre exposed to an Sr-90 source. The trigger is set at 38 mV, it is performed on the signal itself.

The prototype overlap detectors were tested in the lab with an Sr-90 source. The ODs were placed horizontally in a light-tight box; the source was placed on top of the fibres that were connected to a 64-channel MAPMT. A piece of plastic scintillator connected to a PMT was placed under the fibres and was used as trigger counter. The average light yield for the ODs fibres was 1.4 photoelectrons. Under the same conditions the detectors ALFA 2_2_32 and 2_2_64 [1] gave a light yield of 1.3 and 1.4 photoelectrons, respectively. The absolute number of photoelectrons may be not very precise. However the comparison between the three detectors shows that all of them have the same light yield.

The results of the measurements performed on the detectors and the ones performed on the single fibres can not be compared because the two methods are different and do not give absolute numbers but relative information to compare different objects under the same conditions. However these measurements showed that the scintillating fibres did not suffer during the construction of the detector and that it is possible to bend them beyond the specified curvature radius if it is done following a temperature cycle that gently reaches their plastic deformation temperature.

During the month of October 2006 the detectors were tested in a particle beam at CERN. Analysis is ongoing but as a very preliminary result, we can say that online reconstruction of the relative position of one OD with respect to the other was successful. The results matched the measurements performed on the ODs with a mechanical comparator shown in the picture of Figure 18.

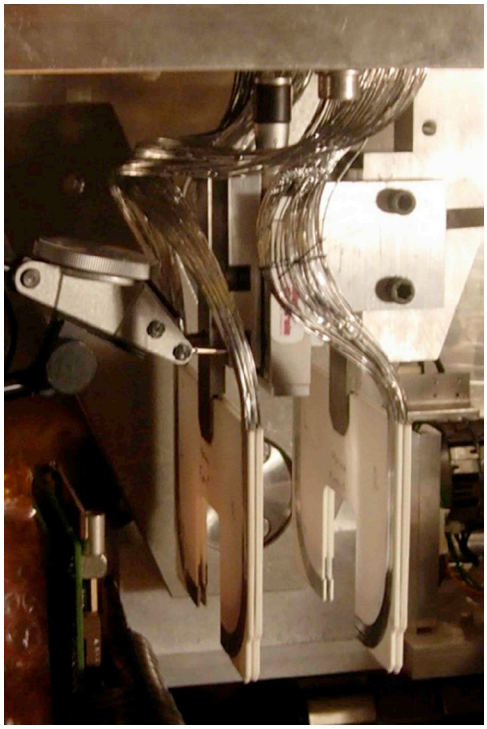

Figure 18: Comparator in contact with OD2 to measure its displacement w.r.t. OD1 during tests in the particle beam.

8. Conclusions

A prototype of the overlap detector for the precise alignment of the ALFA system was built and tested in a high-energy beam at CERN in October 2006. The tests validated the detector concept, the construction method and the temperature treatment developed for the bending of Al-coated scintillating fibres.

We are now going ahead with the final design and we will construct a detector to be tested in a beam by the end of 2007. We hope to be able to integrate the new prototype in a Roman Pot unit.

Acknowledgements

The prototype detector was built at CERN in collaboration with technicians from the universities of Giessen (Germany) and Lisbon (Portugal).

The metrology of the overlap detectors was done at CERN in collaboration with two summer students from the Czech republic. We acknowledge the work of A. Kocnar and J. Pospichal.

References

[1] S. Ask, P. Barrillon, A. Braem, C. Cheiklali, I. Efthymiopoulos, D. Fournier, C. d. L. Taille, B. D. Girolamo, P. Grafstrom, C. Joram, M. Haugenauer, V. Hedberg, B. Lavigne, A. Maio, A. Mapelli, U. Mjörnmark, P. Puzo, M. Rijssenbeek, J. Santos, J. G. Saraiva, H. Stenzel, M. Thioye, E. Valladolid, and V. Vorobel, "Luminosity measurement at ATLAS - Development, Construction and Test of Scintillating Fibre Prototype Detectors," *Nuclear Instruments and Methods in Physics Research Section A: Accelerators, Detectors and Associated Equipment,* vol. 568, pp. 588-600, 1 December 2006 2006.

[2] C. Joram and H. Stenzel, "The Overlap Detectors," 2006.

[3] A. Braem, A. Folley, C. Joram, and L. Kottelat, "Characterization studies on scintillating fibres," CERN, 2006.

[4] J. G. Saraiva and e. al., "Aluminization of scintillating fibers for the luminosity detector of ATLAS," Lisbon CFNUL/FCUL/UL, LIP, CEFI-TEC/FCT/UNL, IPB, 2005.

[5] A. Braem, C. Joram, A. Mapelli, A. Kocnar, and J. Pospichal, "Metrology results of the ALFA 2006 prototype detectors," ATL-LUM-PUB-2006-007, 2006.

Annex

Table 1: Measured geometrical fibre parameters of overlap detectors.

OD	layer	fibre	a (mm)	b (mm)	z (mm)
2	1	1	-0.00450	-144.876	0.000
2	1	2	-0.00460	-144.384	0.000
2	1	3	-0.00470	-143.891	0.000
2	1	4	-0.00450	-143.403	0.000
2	1	5	-0.00460	-142.912	0.000
2	1	6	-0.00450	-142.424	0.000
2	1	7	-0.00470	-141.925	0.000
2	1	8	-0.00530	-141.419	0.000
2	1	9	-0.00530	-140.927	0.000
2	1	10	-0.00490	-140.444	0.000
2	1	11	-0.00490	-139.953	0.000
2	1	12	-0.00520	-139.454	0.000
2	1	13	-0.00460	-138.979	0.000
2	1	14	-0.00440	-138.498	0.000
2	1	15	-0.00450	-138.006	0.000
2	2	1	0.00538	-144.850	0.000
2	2	2	0.00540	-144.361	0.000

OD	layer	fibre	a (mm)	b (mm)	z (mm)
1	9	1	-0.00785	-145.081	5.000
1	9	2	-0.00800	-144.590	5.000
1	9	3	-0.00910	-144.078	5.000
1	9	4	-0.00930	-143.588	5.000
1	9	5	-0.00950	-143.094	5.000
1	9	6	-0.00980	-142.597	5.000
1	9	7	-0.00930	-142.114	5.000
1	9	8	-0.00900	-141.627	5.000
1	9	9	-0.00960	-141.127	5.000
1	9	10	-0.00990	-140.634	5.000
1	9	11	-0.00980	-140.152	5.000
1	9	12	-0.00920	-139.681	5.000
1	9	13	-0.00910	-139.194	5.000
1	9	14	-0.00900	-138.707	5.000
1	9	15	-0.00915	-138.215	5.000
1	10	1	-0.00028	-145.240	5.000
1	10	2	0.00000	-144.745	5.000

2	2	3	0.00450	-143.895	0.000
2	2	4	0.00490	-143.398	0.000
2	2	5	0.00550	-142.893	0.000
2	2	6	0.00520	-142.412	0.000
2	2	7	0.00500	-141.928	0.000
2	2	8	0.00490	-141.440	0.000
2	2	9	0.00490	-140.952	0.000
2	2	10	0.00520	-140.455	0.000
2	2	11	0.00500	-139.972	0.000
2	2	12	0.00470	-139.490	0.000
2	2	13	0.00450	-139.005	0.000
2	2	14	0.00560	-138.489	0.000
2	2	15	0.00562	-138.000	0.000
2	3	1	0.00010	-137.439	0.670
2	3	2	0.00010	-136.950	0.670
2	3	3	0.00040	-136.470	0.670
2	3	4	-0.00040	-135.966	0.670
2	3	5	-0.00110	-135.465	0.670
2	3	6	0.00030	-135.019	0.670
2	3	7	-0.00010	-134.519	0.670
2	3	8	-0.00080	-134.009	0.670
2	3	9	-0.00080	-133.516	0.670
2	3	10	-0.00070	-133.025	0.670
2	3	11	-0.00030	-132.546	0.670
2	3	12	-0.00080	-132.040	0.670
2	3	13	-0.00080	-131.549	0.670
2	3	14	-0.00030	-131.074	0.670
2	3	15	-0.00030	-130.585	0.670
2	4	1	0.00328	-137.467	0.670
2	4	2	0.00340	-136.972	0.670
2	4	3	0.00400	-136.468	0.670
2	4	4	0.00470	-135.968	0.670
2	4	5	0.00430	-135.502	0.670
2	4	6	0.00450	-135.003	0.670
2	4	7	0.00470	-134.497	0.670
2	4	8	0.00470	-133.999	0.670
2	4	9	0.00450	-133.505	0.670
2	4	10	0.00440	-133.007	0.670
2	4	11	0.00510	-132.491	0.670
2	4	12	0.00530	-131.991	0.670
2	4	13	0.00470	-131.514	0.670
2	4	14	0.00470	-131.027	0.670
2	4	15	0.00482	-130.532	0.670
2	5	1	0.00032	-145.188	2.500
2	5	2	0.00020	-144.697	2.500
2	5	3	0.00020	-144.206	2.500
2	5	4	0.00000	-143.716	2.500
2	5	5	-0.00050	-143.221	2.500
2	5	6	-0.00060	-142.731	2.500
2	5	7	-0.00070	-142.240	2.500
2	5	8	-0.00090	-141.747	2.500
2	5	9	-0.00100	-141.258	2.500
2	5	10	-0.00100	-140.768	2.500
2	5	11	-0.00080	-140.279	2.500
2	5	12	-0.00100	-139.789	2.500
2	5	13	-0.00110	-139.300	2.500
2	5	14	-0.00120	-138.803	2.500
2	5	15	-0.00132	-138.312	2.500

1	10	3	0.00070	-144.240	5.000
1	10	4	0.00110	-143.737	5.000
1	10	5	0.00140	-143.241	5.000
1	10	6	0.00180	-142.746	5.000
1	10	7	0.00230	-142.245	5.000
1	10	8	0.00260	-141.750	5.000
1	10	9	0.00260	-141.261	5.000
1	10	10	0.00310	-140.761	5.000
1	10	11	0.00360	-140.262	5.000
1	10	12	0.00300	-139.788	5.000
1	10	13	0.00290	-139.300	5.000
1	10	14	0.00330	-138.804	5.000
1	10	15	0.00358	-138.308	5.000
1	11	1	-0.00578	-137.643	5.670
1	11	2	-0.00570	-137.155	5.670
1	11	3	-0.00530	-136.671	5.670
1	11	4	-0.00520	-136.185	5.670
1	11	5	-0.00530	-135.694	5.670
1	11	6	-0.00550	-135.200	5.670
1	11	7	-0.00570	-134.704	5.670
1	11	8	-0.00570	-134.211	5.670
1	11	9	-0.00560	-133.723	5.670
1	11	10	-0.00510	-133.248	5.670
1	11	11	-0.00520	-132.756	5.670
1	11	12	-0.00530	-132.261	5.670
1	11	13	-0.00500	-131.779	5.670
1	11	14	-0.00490	-131.294	5.670
1	11	15	-0.00482	-130.805	5.670
1	12	1	-0.00102	-137.803	5.670
1	12	2	-0.00050	-137.299	5.670
1	12	3	0.00130	-136.766	5.670
1	12	4	0.00290	-136.239	5.670
1	12	5	0.00360	-135.730	5.670
1	12	6	0.00400	-135.229	5.670
1	12	7	0.00430	-134.728	5.670
1	12	8	0.00450	-134.232	5.670
1	12	9	0.00460	-133.739	5.670
1	12	10	0.00450	-133.251	5.670
1	12	11	0.00450	-132.758	5.670
1	12	12	0.00510	-132.247	5.670
1	12	13	0.00560	-131.747	5.670
1	12	14	0.00580	-131.253	5.670
1	12	15	0.00632	-130.749	5.670
1	13	1	-0.00101	-144.960	7.500
1	13	2	-0.00110	-144.469	7.500
1	13	3	-0.00120	-143.977	7.500
1	13	4	-0.00130	-143.486	7.500
1	13	5	-0.00160	-142.990	7.500
1	13	6	-0.00200	-142.489	7.500
1	13	7	-0.00230	-141.992	7.500
1	13	8	-0.00220	-141.506	7.500
1	13	9	-0.00230	-141.016	7.500
1	13	10	-0.00220	-140.530	7.500
1	13	11	-0.00210	-140.043	7.500
1	13	12	-0.00240	-139.551	7.500
1	13	13	-0.00250	-139.061	7.500
1	13	14	-0.00240	-138.571	7.500
1	13	15	-0.00249	-138.080	7.500

2	6	1	0.00049	-145.183	2.500
2	6	2	0.00080	-144.684	2.500
2	6	3	0.00230	-144.157	2.500
2	6	4	0.00440	-143.613	2.500
2	6	5	0.00440	-143.122	2.500
2	6	6	0.00300	-142.665	2.500
2	6	7	0.00340	-142.166	2.500
2	6	8	0.00360	-141.668	2.500
2	6	9	0.00390	-141.168	2.500
2	6	10	0.00400	-140.675	2.500
2	6	11	0.00420	-140.175	2.500
2	6	12	0.00410	-139.681	2.500
2	6	13	0.00380	-139.199	2.500
2	6	14	0.00390	-138.709	2.500
2	6	15	0.00421	-138.210	2.500
2	7	1	-0.00456	-137.670	3.170
2	7	2	-0.00470	-137.175	3.170
2	7	3	-0.00530	-136.667	3.170
2	7	4	-0.00630	-136.152	3.170
2	7	5	-0.00700	-135.642	3.170
2	7	6	-0.00700	-135.150	3.170
2	7	7	-0.00740	-134.649	3.170
2	7	8	-0.00740	-134.156	3.170
2	7	9	-0.00720	-133.671	3.170
2	7	10	-0.00770	-133.168	3.170
2	7	11	-0.00790	-132.673	3.170
2	7	12	-0.00720	-132.199	3.170
2	7	13	-0.00620	-131.731	3.170
2	7	14	-0.00600	-131.243	3.170
2	7	15	-0.00614	-130.748	3.170
2	8	1	-0.00168	-137.723	3.170
2	8	2	-0.00150	-137.228	3.170
2	8	3	-0.00130	-136.734	3.170
2	8	4	-0.00130	-136.246	3.170
2	8	5	-0.00140	-135.761	3.170
2	8	6	-0.00130	-135.268	3.170
2	8	7	-0.00140	-134.777	3.170
2	8	8	-0.00090	-134.275	3.170
2	8	9	-0.00060	-133.773	3.170
2	8	10	-0.00140	-133.298	3.170
2	8	11	-0.00070	-132.789	3.170
2	8	12	0.00000	-132.280	3.170
2	8	13	0.00020	-131.787	3.170
2	8	14	0.00060	-131.288	3.170
2	8	15	0.00078	-130.792	3.170

1	14	1	-0.00263	-145.019	7.500
1	14	2	-0.00240	-144.525	7.500
1	14	3	-0.00230	-144.032	7.500
1	14	4	-0.00220	-143.541	7.500
1	14	5	-0.00210	-143.047	7.500
1	14	6	-0.00200	-142.556	7.500
1	14	7	-0.00200	-142.071	7.500
1	14	8	-0.00120	-141.564	7.500
1	14	9	-0.00060	-141.063	7.500
1	14	10	-0.00030	-140.573	7.500
1	14	11	-0.00010	-140.080	7.500
1	14	12	0.00030	-139.578	7.500
1	14	13	0.00070	-139.074	7.500
1	14	14	0.00070	-138.585	7.500
1	14	15	0.00093	-138.090	7.500
1	15	1	-0.00037	-137.551	8.170
1	15	2	-0.00100	-137.043	8.170
1	15	3	-0.00310	-136.500	8.170
1	15	4	-0.00480	-135.965	8.170
1	15	5	-0.00520	-135.467	8.170
1	15	6	-0.00540	-134.971	8.170
1	15	7	-0.00550	-134.476	8.170
1	15	8	-0.00600	-133.969	8.170
1	15	9	-0.00660	-133.455	8.170
1	15	10	-0.00730	-132.938	8.170
1	15	11	-0.00830	-132.416	8.170
1	15	12	-0.00880	-131.912	8.170
1	15	13	-0.00840	-131.433	8.170
1	15	14	-0.00850	-130.940	8.170
1	15	15	-0.00913	-130.431	8.170
1	16	1	0.00784	-137.434	8.170
1	16	2	0.00770	-136.938	8.170
1	16	3	0.00770	-136.429	8.170
1	16	4	0.00740	-135.926	8.170
1	16	5	0.00710	-135.428	8.170
1	16	6	0.00730	-134.928	8.170
1	16	7	0.00690	-134.451	8.170
1	16	8	0.00710	-133.957	8.170
1	16	9	0.00760	-133.451	8.170
1	16	10	0.00680	-132.975	8.170
1	16	11	0.00680	-132.475	8.170
1	16	12	0.00680	-131.969	8.170
1	16	13	0.00630	-131.479	8.170
1	16	14	0.00600	-130.987	8.170
1	16	15	0.00586	-130.491	8.170